Bioconjugate Chemistry

Article

pubs.acs.org/bc

Novel Imidazolium Salt–Peptide Conjugates and Their Antimicrobial Activity

A. Reinhardt,[†] M. Horn,[†] J. Pieper gen. Schmauck,[‡] A. Bröhl,[‡] R. Giernoth,[‡] C. Oelkrug,[§] A. Schubert,[§] and I. Neundorf*,[†]

[†]Department of Chemistry, Institute of Biochemistry, University of Cologne, Zuelpicher Str. 47, D-50674 Cologne, Germany

[‡]Department of Chemistry, Organic Chemistry, University of Cologne, Greinstr. 4, D-50939 Cologne, Germany

[§]Fraunhofer Institute for Cell Therapy and Immunology, Perlickstr. 1, D-04103 Leipzig, Germany

Supporting Information

ABSTRACT: Our study presents innovative research dealing with the synthesis and biological evaluation of conjugates out of antimicrobial peptides (AMPs) and imidazolium cations that are derived from ionic liquids. AMPs are considered as promising alternatives to common antibiotics due to their different activity mechanisms. Antibacterial effects have also been described for ionic liquids bearing imidazolium cations . Besides single coupling of carboxy-functionalized imidazolium cations to the peptide N-terminal we also developed conjugates bearing multiple copies of imidazolium cations. The combination of both compounds resulted in synergistic effects that were most pronounced when more imidazolium cations were attached to the peptides. In addition, antibacterial activity even in drug-resistant bacterial strains could be observed. Moreover, the novel compounds showed good selectivity only against bacterial cells, an observation that was further proven by lipid interaction studies using giant unilamellar vesicles.

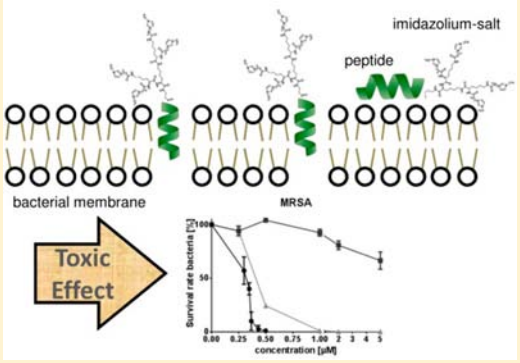

INTRODUCTION

Antimicrobial peptides (AMPs) are a heterogeneous group of antibiotic molecules that are produced by virtually all multicellular organisms, e.g., animals, plants, bacteria, and fungi.[1−3] They are involved in the innate immune defense system[4] where they play a major role in the defense of pathogenic microorganisms. For instance, mammalian AMPs are expressed in epithelial surfaces to repel invasion by bacteria, viruses, fungi, and parasites.[5] AMPs are short-length peptide antibiotics with mostly cationic and amphipathic characteristics.[6] The structural properties of AMPs differ between α-helical, β-sheeted, extended, and looped.[7] Moreover, they are active against a wide spectrum of microorganisms, such as Gram-positive and Gram-negative bacteria, as well as parasites and viruses.[1,8,9] AMPs are cell specific and able to distinguish host from nonhost cells, which is mainly based on differences in cell membrane charge and composition of microbial and mammalian cells.[10] It is proposed that positively charged AMPs strongly interact with the negatively charged cell membrane of the microorganism,[11] leading to an insertion into the hydrophobic core of the cell membrane and formation of trans-membrane channels, which cause a breakdown of the membrane potential subsequently leading to cell death.[12] Moreover, pore and nonpore models are distinguished:[9] pore models promote formation of membrane-spanning pores, containing the barrel-stave model,[13] where the attached peptides aggregate, and as a result form a hydrophilic channel, and the toroidal pore model[14] in which the AMPs affect the curvature of the membrane leading to a pore, which is built from the inserted peptides as well as from the lipid head groups. In turn, nonpore models include the carpet model,[15] where a parallel deposition of AMPs on the membrane like a carpet leads to permeabilization of the cell membrane, and the detergent model[16] that explains a collapse of the membrane due to high AMP concentrations. In addition, some AMPs show an alternative mechanism of action like binding to DNA or inhibiting DNA, RNA, and protein synthesis.[2] However, since in the last decades bacteria have become more and more resistant against conventional antibiotics, AMPs have been recognized especially as promising candidates for replacing conventional antibiotics. Particularly, their unique mechanism of action and low specificity in terms of molecular targets reduces the chance of acquired resistance.[10,17]

Within this study the influence of imidazolium cations on the activity of AMPs was investigated. Inspired by recent observations that imidazolium cations, when part of so-called ionic liquids, exhibit biological activity,[18] we wondered if covalent or noncovalent combination with AMPs would lead to

Received: July 24, 2014
Revised: November 24, 2014
Published: November 27, 2014

   dx.doi.org/10.1021/bc500510c | *Bioconjugate Chem.* 2014, 25, 2166−2174

mixtures with improved antimicrobial activity. To our knowledge no study exists that investigates the interplay and biological activity of such compositions.

The two AMPs used in this work are the sC18 and the LL-37 peptide. sC18 is a short C-terminal fragment of the cationic antimicrobial peptide cathelicidin, namely, CAP18, which binds lipopolysaccharide (LPS).[19] sC18 was developed in our group as a cell-penetrating peptide, and uptake via endocytosis was demonstrated.[20] Furthermore, we used sC18 as an efficient delivery system for cytostatic drugs[21,22] as well as for imaging probes.[23,24] In all these studies sC18 itself behaved nontoxically to human cells; however, antimicrobial activity in the micromolar range against *Escherichia coli* and *Micrococcus luteus* has been observed (unpublished results). The LL-37 peptide also belongs to the group of cathelicidins and is a two amino acid truncated form of FALL-39,[25] which was identified as an antimicrobial peptide expressed in bone marrow. LL-37 shows activity against a wide spectrum of Gram-negative and Gram-positive bacteria, and its mechanism of action is proposed to follow the carpet-like mechanism.[26]

RESULTS AND DISCUSSION

Synthesis of Imidazolium Cation−AMP Conjugates. The ionic liquids investigated in this study consist of 1-alkyl-3-methylimidazolium [$C_{alkyl}C_{1im}$] based cations and bromide as anion. The IL precursors, as well as compound **4c** that was used as a reference substance, were synthesized in close analogy to the recent literature.[27,28] Details can be found in the Supporting Information.

All peptides were synthesized by solid phase peptide synthesis (SPPS) according to the Fmoc/tBu-strategy on a Rink amide resin. The carboxy-functionalized imidazolium salts **4a** and **4b** were coupled at the N-terminus of the peptides when still bound to the solid support using HATU and DIPEA as the activating reagent (Figure 1a).

To increase the payload of imidazolium compounds a branched linker structure based on three lysine residues was designed (see Figure 1b). Furthermore, conjugates **3b** and **3c** were additionally labeled with the fluorophore 5,6-carboxyfluorescein at the ε-lysine side chain as indicated in Figure 1. Additionally, unmodified peptides **1a** and **2a** were synthesized and used as control peptides. All peptides were cleaved from the resin by the addition of trifluoroacetic acid and precipitated in diethyl ether. After purification using preparative HPLC, all compounds are present as trifluoroacetate salts. Table 1 shows the analytical results of the imidazolium salt−peptide conjugates that have been all clearly identified by ESI MS.

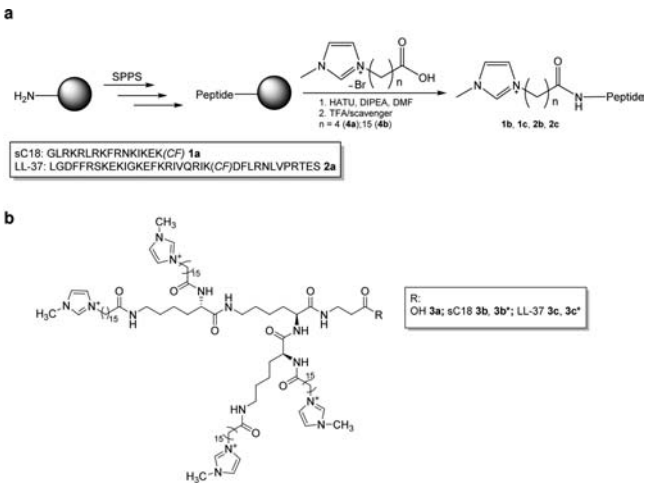

Figure 1. (a) Imidazolium salt−peptide conjugates were synthesized via SPPS. After cleavage from the resin the new compounds exist as trifluoroacetate salts. (b) Structure of **3b**, **3b***, **3c**, and **3c*** bearing four imidazolium cations. *CF*: peptides are labeled with 5(6)-carboxyfluorescein at the ε-amino group of lysine at the indicated positions. Refer also to Table 1.

Secondary Structure Determination. First we determined the secondary structure of compounds **1a−1c**, **2a−2c**, **3b**, and **3c** to see if there would be any structural influence of the imidazolium compounds to the peptides. Therefore, peptides were dissolved in 10 mM phosphate buffer as well as in 10 mM phosphate buffer with the addition of 50% trifluorethanol (TFE) (a secondary structure-inducing reagent) and analyzed using circular dichroism spectroscopy (Figure 2). Peptides **1a−1c** and **3b** displayed a random coil conformation in 10 mM phosphate buffer, pH 7 (Figure 2a), with minima around 200 nm. The addition of 50% TFE induced an α-helical conformation with positive bands around 192 nm and two minima at 222 and 207 nm (Figure 2c). For peptide **1a**, the parent sC18 peptide, the results agree with recently published data.[20] Peptides **2a−2c** and **3c** displayed α-helical structure in 10 mM phosphate buffer, pH 7, as well as in the presence of TFE (Figure 2b,d), again with positive bands around 192 nm and minima at 222 and 207 nm. For LL-37 itself as well as for derivatives of LL-37 the formation of α-helical structures has already been reported.[26] However, the spectra were further analyzed concerning the α-helical content in the conjugates by calculating the ratio between the molar ellipticity at 222 and 207 nm (R = [θ]222 nm/[θ]207 nm).[30] The R values demonstrate that the attached imidazolium compounds have no significant influence on the formation of the α-helical structure. In addition, we tested exemplarily if there would be any conformational shifts when incubating peptide **3c** in 10 mM phosphate buffer with 50% TFE at different pH values (Supporting Information, Figure S1). The R-values obtained demonstrated that both an acidic as well as a basic milieu did not affect the secondary structure of the peptide.

Antimicrobial Activity Studies. Antibacterial activity of all conjugates was investigated against a range of various bacteria, including clinically resistant microbes. In more detail, we employed a Gram-positive bacterium (*Bacillus subtilis*), a Gram-negative bacterium (*Escherichia coli*), and an acid-fast bacterium (*Mycobacterium phlei*), as well as vancomycin-resistant *Enterococcus* sp. (VRE) and methicillin-resistant *Staphylococcus aureus* (MRSA). The minimum inhibitory concentration that inhibits 50% of bacterial isolates (MIC_{50})[31] was determined and manually deduced from the individual graphs for each compound tested (Supporting Information, Figure S2). The values are depicted in Table 2. As control substances we used the unmodified peptides **1a** and **2a**, as well as gentamycin, streptomycin, and tetracycline as commonly used antibiotics.[32−34] Although **4c** has been recently shown to exhibit antibacterial activity in the micromolar range (MIC: 0.125−32 μg/mL[18]), we tested it again in our setup and compared it to substances **4a** and **4b**. The obtained results indicate that **4c** has the strongest toxic effect against all bacterial strains tested (Table 2). The other two ionic liquids **4a** and **4b** bearing a carboxylic acid for coupling to the AMPs showed no toxic effect at all against *E. coli* and *B. subtilis* within the concentration range tested. Furthermore, the toxicity of **4a** and **4b** on *M. phlei*

dx.doi.org/10.1021/bc500510c | *Bioconjugate Chem.* 2014, 25, 2166−2174

Table 1. Analytical Data of All New Conjugates

name	number	MW_{exp}	MW_{calc}
sC18	**1a**	2069.5	2069.6
$[(CO_2H)^4C_4C_1im]$-sC18	**1b**	2234.8	2234.8
$[(CO_2H)^{15}C_{15}C_1im]$-sC18	**1c**	2388.7	2389.1
LL-37	**2a**	4491.7	4492.4
$[(CO_2H)^4C_4C_1im]$-LL-37	**2b**	4657.0	4657.6
$[(CO_2H)^{15}C_{15}C_1im]$-LL-37	**2c**	4811.8	4811.9
$[[(CO_2H)^{15}C_{15}C_1im]Lys[(CO_2H)^{15}C_{15}C_1im]$-Lys(&)-$\beta$Ala] $[[(CO_2H)^{15}C_{15}C_1im]Lys[(CO_2H)^{15}C_{15}C_1im]$&]^a	**3a**	1751.5	1751.7
$[[(CO_2H)^{15}C_{15}C_1im]Lys[(CO_2H)^{15}C_{15}C_1im]$-Lys(&)-$\beta$Ala-sC18] $[[(CO_2H)^{15}C_{15}C_1im]Lys[(CO_2H)^{15}C_{15}C_1im]$&]	**3b**	3802.8	3803.3
$[[(CO_2H)^{15}C_{15}C_1im]Lys[(CO_2H)^{15}C_{15}C_1im]$-Lys(&)-$\beta$Ala-sC18(*CF*)] $[[(CO_2H)^{15}C_{15}C_1im]Lys[(CO_2H)^{15}C_{15}C_1im]$&]	**3b***	4160.9	4161.6
$[[(CO_2H)^{15}C_{15}C_1im]Lys[(CO_2H)^{15}C_{15}C_1im]$-Lys(&)-$\beta$Ala-LL-37] $[[(CO_2H)^{15}C_{15}C_1im]Lys[(CO_2H)^{15}C_{15}C_1im]$&]	**3c**	6224.5	6226.1
$[[(CO_2H)^{15}C_{15}C_1im]Lys[(CO_2H)^{15}C_{15}C_1im]$-Lys(&)-$\beta$Ala-LL-37(*CF*)] $[[(CO_2H)^{15}C_{15}C_1im]Lys[(CO_2H)^{15}C_{15}C_1im]$&]	**3c***	6584.5	6584.4
Imidazolium salts			
$[(CO_2H)^4C_4C_1im][Br]$	**4a**		236.13
$[(CO_2H)^{15}C_{15}C_1im][Br]$	**4b**		417.42
$[C_{16}C_1im][Br]$	**4c**		307.54

^{a}According to ref 29. ^{b}* = Peptides are fluorescently labeled with 5(6)-carboxyfluorescein (*CF*).

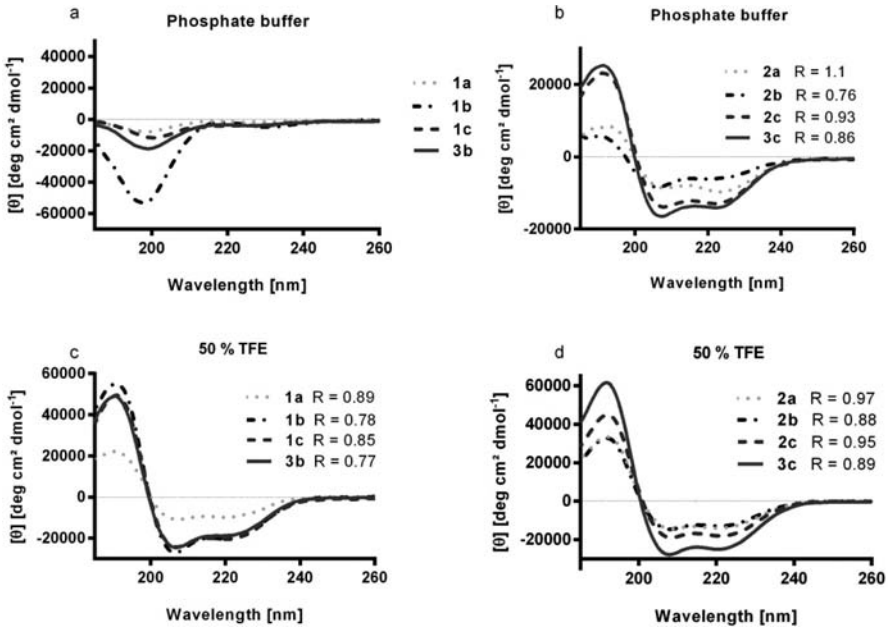

Figure 2. Circular dichroism spectra of the synthesized conjugates. The spectra were measured at a concentration of 20 μM in 10 mM phosphate buffer (a, b) and 10 mM phosphate buffer with 50% TFE (c, d). *R*-values (R) represent the ratio between the molar ellipticity values at 222 and 207 nm.

is five times lower than the toxic effect of the **4c** compound. Therefore, in the following experiments, **4c** was used as a control compound.

However, the novel conjugates were tested within a concentration range of 0−5 μM. Interestingly, when looking at the new compounds **1b** and **1c**, as well as at **2b** and **2c** no significant improved toxic effect against *E. coli* compared to **1a** and **2a** was observed. Moreover, only low antibacterial activity of **1a** and **2a** could be observed (MIC_{50} > 5 μM). Toxic effects against *B. subtilis* were also not detectable for compounds **1a** and **1b**, whereas **1c** displayed some toxicity toward this Gram-positive strain (MIC_{50} = 4−5 μM) (Table 2 and Supporting Information). In contrast to that, all LL-37 based peptides were highly active against this strain, whereby **2c** showed higher activity (MIC_{50} = 1.5 μM) toward *B. subtilis* compared to **2a** and **2b** (MIC_{50} = 2.5−3 μM). Since LL-37 has a more defined amphipathic α-helical structure (what we already observed by CD spectroscopy measurements), it can be assumed that the LL-37 peptides can better integrate into the more compact peptidoglycan layers of *B. subtilis* compared to sC18 and its variants. **2c** seemed to have an especially high antibacterial effect against *B. subtilis*, since at 4 μM only 5% of all bacteria were still alive. Furthermore, we observed that the longer the C-chain of the imidazolium compounds attached, the higher their toxic activity. This phenomenon has been described already for the antibacterial activity of similar imidazolium salts.[35] Interestingly, the acid fast bacterium *M. phlei* was the bacterium most affected after incubation with compounds **1a**−**1c** and **2a**−**2c**, respectively (MIC_{50} = 0.25−5 μM). This was rather unexpected because these bacteria are normally not affected by antibiotic treatment due to their complex myolic acid layer.[36] Again, for the LL-37 series no improvement to compound **2a** was observed. However, conjugate **1c** showed the strongest activity exhibiting an MIC_{50} value of 0.25 μM

dx.doi.org/10.1021/bc500510c | *Bioconjugate Chem.* 2014, 25, 2166−2174

Table 2. Minimal Inhibitory Concentration (MIC_{50}) of All New Synthesized Conjugates[a]

	organism (MIC_{50} [μM])				
compound	*B. subtilis* (ATTC 6633)	*E. coli* K12 (MG 1625)	*M. phlei* (DSM 48214)	VRE	MRSA
1a	-	5	5	>5	>5
1b	-	-	5	n.d.	n.d.
1c	4−5	-	0.25	n.d.	n.d.
2a	3	5	1	0.9	2.3
2b	2.5	-	0.4	n.d.	n.d.
2c	1.5	-	2−3	n.d.	n.d.
3a	1.1	2.5	5	0.5	0.4
3b	0.5	1	0.25	0.2	0.32
3c	1.75	3.5	0.75	0.25	0.6
4a	≫400	≫400	≫400	n.d.	n.d.
4b	≫60	≫60	≫60	n.d.	n.d.
4c	33	20	17	n.d.	n.d.

[a] MIC_{50} values of control compounds: gentamicin (*B. subtilis* 2.1 μM), tetracycline (*E. coli* 32.8 μM), and streptomycin (*M. phlei* 17 μM). -: no activity at the highest concentration tested (5 μM). n.d.: not determined.

(Table 2). Notably, for nearly all compounds it seemed that an increased peptide concentration did not change the antibacterial activity level assuming a bacteriostatic mechanism in this strain (Supporting Information Figure S2).

In the next set of experiments the antimicrobial activity of the covalently coupled imidazolium salt-AMPs was compared to that of the individual mixtures of both components. Until now, there has been no study performed that investigates pure combinations of biologically active peptides, e.g., AMPs, with ionic liquids. Therefore, solutions of different peptide concentrations (0.25−5 μM) and the respective imidazolium salts **4a** and **4b** (2.5 μM) were prepared and incubated with the microorganisms for 6 h. The results are shown in Table S1 (Supporting Information), indicating that for *E. coli* no changes between coupled and uncoupled combinations were detectable. However, results of *B. subtilis* and *M. phlei* showed that incubation with compounds **1c**, **2b**, and **2c** leads to lower MIC_{50} values compared to the uncoupled variants. Especially **2b** and **2c** exhibited more pronounced activity pointing to synergistic effects of both compounds when covalently coupled.

However, since coupling of **4b** seemed to be more promising in this approach, we designed further conjugates bearing at least four imidazolium moieties of this type. To realize this we introduced a branched linker structure based on three lysine residues (see Figure 1b). Together with the branched linker peptide **3a** as control, we tested the new compounds **3b** and **3c** again against *B. subtilis*, *E. coli*, and *M. phlei* (Figure 3). Antibacterial activity was already detectable for the control compound **3a** (MIC_{50} = 1.1−5 μM) with *B. subtilis* being again the most sensitive strain (Figure 3a). Notably, conjugate **3b** based on the sC18 peptide exhibited highly increased activity compared to the LL-37 derived conjugate **3c**. **3b** showed superior activity in all strains over the other compounds. (Figure 3) (MIC_{50} = 0.25−1 μM). In contrast, **3c** was much less active against *B. subtilis* and *E. coli*. Again, the results were different when incubating *M. phlei* with **3a**−**3c**. Here, the minimal inhibitory concentration at which 25−50% of all bacterial isolates were killed was reached relatively quickly, but no changes of activity could be detected even after an increased concentration of the conjugates, an observation similar to the one described before (see Table 2 and Supporting Information).

In summary, peptides **3a**, **3b**, and **3c** displayed a significantly higher toxic effect against *B. subtilis* and *E. coli* compared to **1b**, **1c**, **2b**, and **2c**. For *M. phlei* no further improvement was observed. However, interestingly, all new conjugates exhibited highly improved MIC_{50} values compared to conventional antibiotics (Table 2). Compound **3b** exhibited especially

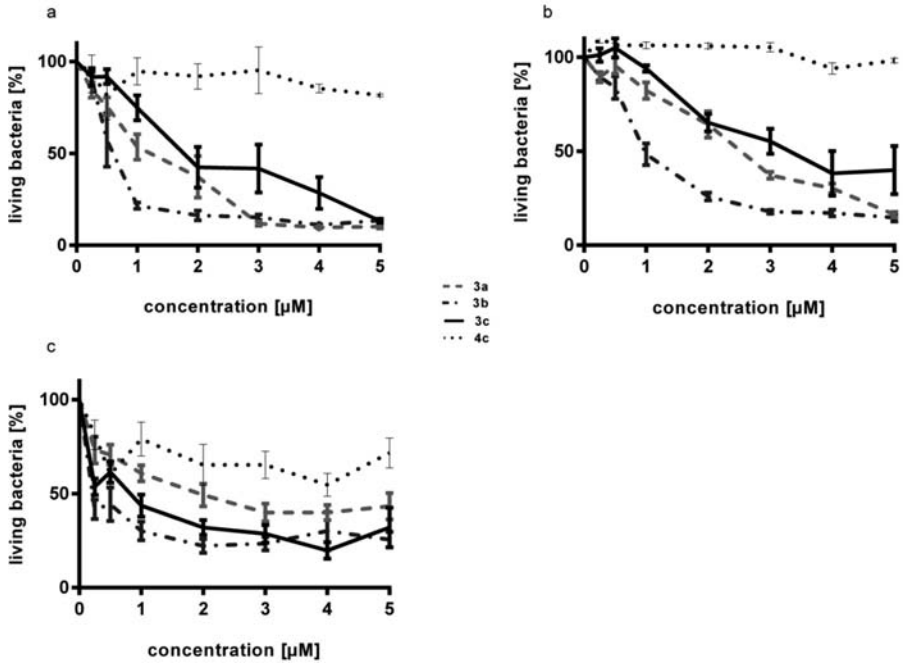

Figure 3. Antimicrobial activity of **3a**−**3c** against *B. subtilis* (a), *E. coli* (b), and *M. phlei* (c). Each value represents the mean ± SEM of nine independent determinations.

dx.doi.org/10.1021/bc500510c | *Bioconjugate Chem.* 2014, 25, 2166−2174

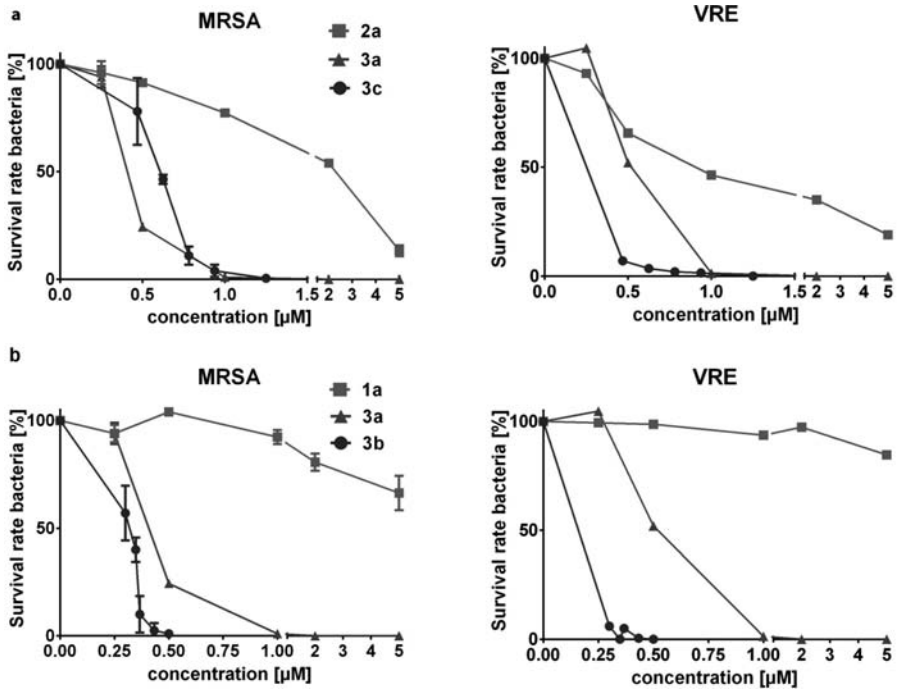

Figure 4. Antimicrobial activity of **3a**–**3c** against vancomycin-resistant enterococci and methicillin-resistant *Staphylococcus aureus*, including (a) LL37 (**2a**) and (b) sC18 (**1a**) as control peptides. Each value represents the mean ± SEM of nine independent determinations.

promising MIC_{50} values for all bacterial strains tested (Table 2). This might be due to the fact that the ramifications of **3b** together with the shorter peptide sequence compared to **2a** provide a better integration into the cell membrane.

Finally, we determined the activity of **3a**–**3c** against vancomycin-resistant enterococci (VRE) and methicillin-resistant *Staphylococcus aureus* (MRSA) (Figure 4). As a control we analyzed the parent AMPs **1a** and **2a**, too. Notably all conjugates exhibited very promising activities with MIC_{50} values in the low micromolar range (0.2–0.6 μM) (Table 2). Again, **3b** displayed slightly higher activities than **3c** and was also more active as compound **3a**. An especially high toxic effect against VRE bacteria with 95% toxicity at 0.2 μM for the **3b** peptide and 0.25 μM for the **3c** peptide was observed.

Hemolytic Activity Studies. We also determined the hemolytic activity of the new compounds against human erythrocytes. Thus, the minimal concentration of each compound required for 50% lysis of human red blood cells (h-RBCs), HC_{50}, was determined. Antimicrobial peptides **1a** and **2a** showed no detectable hemolytic activity (Figure 5) in the concentration range tested. LL-37 was described as non-cell-selective by Oren et al.; however, the concentrations tested in that study were much higher.[26] However, all conjugates having four imidazolium cations attached display increasing hemolytic activity, whereby the effect is most pronounced for compound **3c** (HC_{50} of 2.1 μM) and less developed for **3a** (only around 10% lysis at 5 μM). The observed low selectivity of **3c** might be due to its higher hydrophobicity that is correlated to stronger hemolytic activity.[37] In addition, the presence of the four imidazolium cations might support the non-cell-selectivity of this AMP. In fact **3b** exhibits a HC_{50} of 4.5 μM, but since the activity against the bacterial strains tested is measured at clearly lower concentrations (MIC_{50} 0–1 μM) we can also conclude good selectivity for this compound. Accordingly, the therapeutic index between **3a** and **3b** is not that different (when comparing the ratio between HC_{50} to MIC_{50}), suggesting that **3a** might already be a promising antimicrobial lead structure.

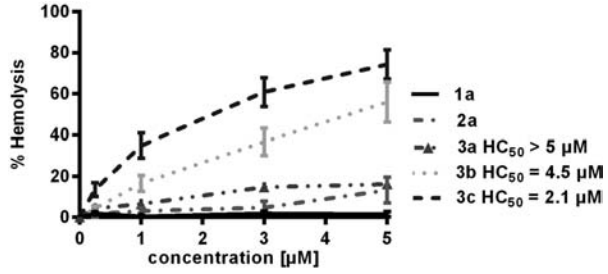

Figure 5. Hemolytic activity of the new peptide conjugates against human red blood cells ($n = 2$). % hemolysis = [($A_{550\ nm}$ of erythrocytes plus peptide − $A_{550\ nm}$ of erythrocytes in PBS)/($A_{550\ nm}$ of erythrocytes in 0.1% Triton-X 100 − $A_{550\ nm}$ of erythrocytes in PBS] × 100.

Investigating Lipid Interaction. AMPs act most likely via nonspecific membrane disturbing processes than by specific interaction with protein targets. They are mostly attracted by electrostatic interactions with the acidic bacterial membrane. However, this membrane interaction can be impaired by the presence of cholesterol in eukaryotic cell membranes.[38] For instance, in erythrocytes more than 60% cholesterol is present in the cell membrane.[39] Cholesterol increases membrane cohesion and membrane stiffness leading to liquid ordered domains that prevent membrane bending and soaking of AMPs. Thus, liquid disordered domains that allow membrane disintegration are phase separated, and overall the activity of AMPs is reduced. Therefore, to get more insight into the mechanism of action of both conjugates, **3b** and **3c**, we performed peptide–lipid interaction studies using giant unilamellar vesicles (GUVs) and assessment by confocal laser scanning microscopy. We composed GUVs with different amounts of cholesterol present (ranging from 20 to 60 mol

dx.doi.org/10.1021/bc500510c | *Bioconjugate Chem.* 2014, 25, 2166–2174

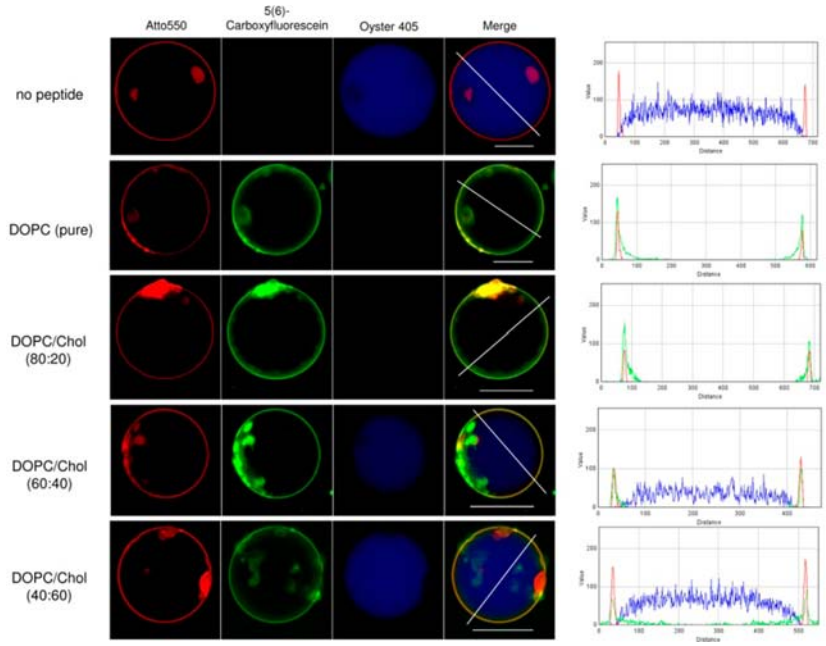

Figure 6. GUV assay with **3b*** and different DOPC/Cholesterol compositions. Respective GUVs were incubated with peptide conjugate (5 μM) for 90 min and analyzed by CLSM. The time at which peptide solutions were added was defined as time zero. The panels on the right side represent the intensity profiles of Atto550 (red), 5,6-carboxyfluorescein (green), and Oyster 405 (blue) along the lines on the confocal pictures on the left. All GUVs contain 0.2 mol % Atto550-DOPE as lipid marker and were loaded with 5 μM Oyster 405. Scale bars, 30 μm.

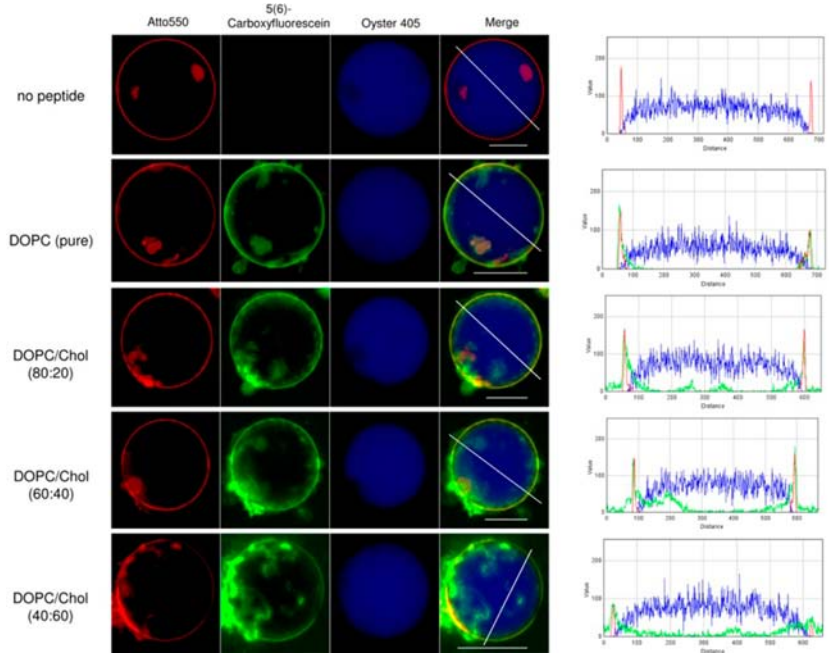

Figure 7. GUV assay with **3c*** and different DOPC/Cholesterol compositions. Respective GUVs were incubated with peptide conjugate (5 μM) for 90 min and analyzed by CLSM. The time at which peptide solutions were added was defined as time zero. The panels on the right side represent the intensity profiles of Atto550 (red), 5,6-carboxyfluorescein (green), and Oyster 405 (blue) along the lines on the confocal pictures on the left. All GUVs contain 0.2 mol % Atto550-DOPE as lipid marker and were loaded with 5 μM Oyster 405. Scale bars, 30 μm.

%).[40] GUVs were generated containing pure 1,2-dioleoyl-*sn*-glycero-3-phosphocholine (DOPC) doped with 0.2 mol % Atto550 labeled 1,2-dioleoyl-*sn*-glycero-3-phosphoethanolamine (DOPE) to visualize their membranes. Furthermore, we encapsulated the dye Oyster 405 to visualize membrane leakage by dye outflow. Compounds **3b** and **3c** were additionally labeled with the fluorophor 5,6-carboxyfluorescein (see Table 1 and Experimental Procedures for details). Figure 6 shows GUVs that were incubated with a 5 μM solution of **3b***. Strong interaction with the lipid phase is visible and proven by intensity profiles. Obviously, complete dye outflow has occurred, suggesting pore-forming events. Since the fluorescent intensity of **3b*** in the surrounding buffer is roughly equal to the intensity in the interior of the vesicles, it can be concluded that the molecules have equilibrated across the vesicle membranes. However, after increasing the cholesterol content

dx.doi.org/10.1021/bc500510c | *Bioconjugate Chem.* 2014, 25, 2166−2174

stepwise up to 60 mol %, a significant decrease in dye outflow is observable. This is in quite good agreement to the hemolytic activity for this compound and demonstrates the protective effect of cholesterol. By investigation of compound **3c***, it seems that besides strong lipid interactions similar to that observed with **3b***, no disrupting membrane events occur, since almost no dye leakage was observed (Figure 7). The intensity profiles showed some green fluorescence inside the vesicles, suggesting that **3c***, at least to some amount, is capable of getting inside the vesicles. Since hemolytic activity was high and, thus, selectivity was only poor for **3c**, these findings might point to a different mechanism of action of this compound compared to **3b**. For LL-37 itself, a carpet-like membrane disintegration has been proposed[26] and our findings are in quite good agreement to this model.

To summarize, the higher activity of **3b** compared to that of **3c** may be due to different membrane activities, whereby for **3b** pore-forming mechanisms seem to play the major role of action. However, by changing the membrane composition these events can be reduced.

CONCLUSION

In conclusion, we investigated for the first time the biological activity of combinations of imidazolium cations derived from ionic liquids with antimicrobial peptides. We found that coupling of imidazolium cations leads to highly potent new compounds with promising antibacterial activity that also show importance against drug-resistant strains. Notably, biological activity is increased after covalent coupling of imidazolium cations. Pure mixtures of AMPs and ILs exhibited no improved effects. Moreover, increased payload also led to higher activities. In this respect, the short peptide **3a** already exhibited highly promising activity, and could thus function as a future lead structure. Furthermore, selectivity studies demonstrated higher activity against bacterial cells. This observation may be due to the different membrane compositions in bacterial and eukaryotic cells, whereby the cholesterol content might be a critical factor.

EXPERIMENTAL PROCEDURES

Solid Phase Peptide Synthesis. **1a** and **2a** were synthesized on Fmoc-Rink amide resin beads (substitution 0.48 mmol/g, 0.015 mmol scale) using an automated peptide synthesizer from MultiSynTech. The peptide coupling was performed as double coupling steps using DIC and Oxyma pure. To the antimicrobial peptides the ionic liquids $[(CO_2H)^4C_4C_1im]Br^-$ and $[(CO_2H)^{15}C_{15}C_1im]Br^-$ (5 equiv) were coupled manually using HATU (5 equiv) and DIPEA (5 equiv) in DMF. For synthesis of **3a** Fmoc-L-βAla was coupled to Fmoc-Wang resin beads (substitution 1.1 mmol/g, 0.22 mmol scale) and the Fmoc protecting group was removed with piperidine (20% in DMF, 5 min followed by 20% in DMF, 15 min). Fmoc-L-Lys(Fmoc)-OH (3 equiv) was attached using HATU (3 equiv) and DIPEA (3 equiv). Afterward Fmoc-L-Lys(Fmoc)-OH and $[(CO_2H)^{15}C_{15}C_1im]Br^-$ were coupled using the same coupling protocol as indicated above. Synthesis of **3b** and **3c** was started with synthesis of the antimicrobial peptides via an automated peptide synthesizer. The further synthesis steps were equal to the synthesis of **3a**. After each coupling a capping step was performed with Ac_2O/DIPEA (10:10 equiv in DMF, 15 min). For fluorescence labeling peptides **3a*** and **3b***, 5(6)-carboxyfluorescin (CF) (3 equiv) was coupled with HATU (3 equiv) and DIPEA (3 equiv) at lysine side chains of the antimicrobial peptides for 3 h. CF-labeled peptides were used for experiments with giant unilamellar vesicles. Control peptides were synthesized using an automated peptide synthesizer. In all cases the synthesis progress was monitored by RP HPLC ESI-MS and ninhydrin colorimetric test.

Peptides were removed from the resin using TFA/TIS/H_2O (95:2.5:2.5 v/v/v) for 3 h and precipitated in ice-cold diethyl ether. Peptides were purified using preparative RP HPLC and fractions were analyzed by analytic RP HPLC ESI-MS. Peptide containing fractions were combined and lyophilized. Final purity of all compounds was >95%.

Circular Dichroism Spectroscopy. All CD spectra were measured with the Jasco Corp J715 spectrometer at 20 °C using a 0.1-cm-thick quartz cell. The spectra were recorded in the range 180−260 nm in 0.2 nm intervals, 1 nm bandwidth, four accumulations, sensitivity 100 mdeg, and 50 nm/min scanning speed. Twenty micromolar peptide concentrations were used in 10 mM phosphate buffer, pH 7.0, or 10 mM phosphate buffer/TFE (1:1 v/v), pH 7.0.

Antimicrobial Activity. For antimicrobial activity tests a Gram-positive (*Bacillus subtilis* (ATTC 6633)), Gram-negative (*Escherichia coli* K12 (MG 1625)), and acid-fast (*Mycobacterium phlei* (DSM 48214)) bacterial strain was used. The bacteria were cultured in Mueller-Hinton Broth (MHB) for 12 h at 30 °C up to an OD_{600} of 0.7. The new conjugates were added to the first horizontal row in the 96-well plate and diluted with water to contain three replicates and seven different concentrations for each tested combination. In each well 180 μL MHB and 10 μL of bacteria suspension were added. As a positive control gentamicin (for *Bacillus subtilis*), streptomycin (for *Mycobacterium phlei*), and tetracyclin (for *Escherichia coli*) were used while aqua bidest was used as negative control. Microbial growth was determined after incubation for 6 h at 30 °C with the iodnitrotetrazoliumpurple (INT) assay (iodnitrotetrazolium-chloride 1 mg/mL in DMSO, 30 min at 30 °C).[41] The 96-well plate was subsequently put in an ELISA plate reader to measure the MIC_{50} value (peptide concentration where only 50% of the bacteria are still alive) at 540 nm. Negative control was set up to 100%.

Preparation of Giant Unilamellar Vesicles (GUVs). 1,2-Dioleoyl-*sn*-glycero-3-phosphocholine (DOPC) was purchased from Avanti Polar Lipids (Alabaster, USA) and Atto550 labeled 1,2-dioleoyl-*sn*-glycero-3-phophoethanolamine (DOPE) was from Atto Tec (Siegen, Germany). Cholesterol was obtained from Sigma-Aldrich (Taufkirchen, Germany). GUVs were prepared as described previously[42,43] with minor modifications. First, super low melting agarose (1% w/v) was coated on a clean glass slide and dried on a hot plate (~50 °C) for 30 min. Afterward, two droplets of the respective lipid solutions (10 μL each) were spread on the agarose film and dried *in vacuo* for at least 1 h to remove residual chloroform. Then, a seal ring was placed onto the lipid coated areas on the slide to obtain two sealed chambers. For the preparation of GUVs encapsulating Oyster 405 (725 Da, Luminaris GmbH, Münster, Germany), a buffer containing 10 mM HEPES; pH 7.4, 50 mM KCl, 50 mM NaCl, 1 mg/mL dextran (from *Leuconostoc* spp., 6 kDa) and 5 μM Oyster 405 (300 μL each) was added to the hybrid film. The glass slide was then left in the dark for 2 h to allow hydration and swelling of the lipids. To harvest the GUV suspension, the glass slide was gently tilted in all directions to detach the liposomes from the surface. The giant liposomes

were then stored in LoBind tubes (1.5 mL, Eppendorf, Hamburg, Germany) at room temperature and used within 3 days.

CLSM Observations of GUVs Treated with Peptide Conjugates. Giant unilamellar vesicles loaded with the membrane-impermeant fluorophore Oyster 405 were prepared as described before. To remove untrapped Oyster 405, liposomes were centrifuged two times at 14 000 × *g* at room temperature for 10 min (Heraeus Pico 17 centrifuge, Thermo Scientific, Germany). A 40 μL aliquot of the GUV solution was diluted in 50 μL of the respective buffer without Oyster 405 and was then transferred into a tissue culture vessel (FlexiPERM slide, 8 wells, Sarstedt, Germany). CF labeled peptide conjugates diluted in buffer containing 10 mM HEPES; pH 7.4, 50 mM KCl, 50 mM NaCl, 1 mg/mL dextran (from *Leuconostoc* spp., 6 kDa) were added to the outer solution of GUVs at a final concentration of 5 μM.

The GUV−peptide interaction was analyzed using a confocal laser scanning system (Nikon D-Eclipse C1) consisting of an inverted microscope (Nikon Eclipse Ti) equipped with a 20× objective (NA 0.45, Plan Fluor; Nikon). Microscope pictures were recorded in 16-bit grayscale, pseudocolored in red (channel 1), green (channel 2), and blue (channel 3) followed by processing with ImageJ. The fluorescence intensity was determined using ImageJ as well.

Hemolytic Activity. The hemolytic activity of the peptide conjugates against human red blood cells (h-RBCs) was determined based on the release of hemoglobin. H-RBCs (received from healthy volunteers) were harvested by 5000*g* at 4 °C for 10 min and washed three times with phosphate-buffered saline (PBS) by centrifugation at 1000*g* at 4 °C for 10 min and resuspended in PBS. Peptide solutions were added to 50 μL of h-RBCs in PBS to a final volume of 100 μL and a final h-RBCs concentration of 4%, v/v. The solution was shaken at 37 °C for 60 min and then centrifuged at 1000*g* for 5 min. The supernatant was added in 96-well plates and the released hemoglobin measured at 550 nm. Zero percent hemolysis was defined as that observed in PBS; 100% was defined as that observed in 0.1% (v/v) Triton X-100. Percentage of hemolysis was calculated: % hemolysis = $[(A_{550\ nm}$ of erythrocytes plus peptide $- A_{550\ nm}$ of erythrocytes in PBS$)/(A_{550\ nm}$ of erythrocytes in 0.1% Triton-X 100 $- A_{550\ nm}$ of erythrocytes in PBS$] \times 100$.

Killing Assay. The killing assay was performed against vancomycin-resistant enterococci and methicillin-resistant *Staphylococcus aureus*.

For enterococci experiments bacteria were cultured in Trypticase-Soja-Bouillon and plated. Killing assays for VRE were performed after an overnight culture was adjusted to an OD_{600} of 0.05 in a 1000 μL Trypticase-Soya-Bouillon and incubated at 37 °C and 1000 rpm for 2 h. After reaching an OD_{600} value of 0.3, the bacteria suspension was diluted to 700 cfu/180 μL in 10 mM PPB and 0.5% LB-media. 180 μL of this dilution was transferred to 20 μL of the peptide solutions at different concentrations (**3b**/**3c**). These settings were shaken at 600 rpm at 37 °C for 1 h and plated on Bacto Brain Heart Infusion (BD) Agar plates. After incubation at 37 °C overnight, the grown bacteria colonies were counted.

For MRSA experiments bacteria were cultured in LB Broth, Lennox (Acumedia), and plated on LB-Agar plates. Killing assays for MRSA were performed after an overnight culture was adjusted to an OD_{600} of 0.1 in a 1000 μL Trypticase-Soya-Bouillon and incubated at 37 °C and 1000 rpm for 1 h. After reaching an OD_{600} value of 0.3 the bacteria suspension was diluted to 500 cfu/180 μL in 10 mM PPB and 2% LB-media. 180 μL of this dilution was transferred to 20 μL of the peptide solutions at different concentrations (**3b**/**3c**). The mixtures were shaken at 600 rpm at 37 °C for 1 h and plated on LB-Agar plates. After incubation at 37 °C overnight, the grown bacteria colonies were counted.

■ ASSOCIATED CONTENT

Ⓢ Supporting Information

Additional information as noted in the text (Table S1, Figure S1−S2, synthesis of compounds **4a**−**4c**). This material is available free of charge via the Internet at http://pubs.acs.org.

■ AUTHOR INFORMATION

Corresponding Author

*E-mail: ines.neundorf@uni-koeln.de. Phone: +49 (0) 221 470 8847. Fax: +49 (0) 221 470 6431.

Notes

The authors declare no competing financial interest.

■ ACKNOWLEDGMENTS

We kindly thank A. Hochheiser for help with LC-MS and N. Pietzsch for the cultivation and killing assays. R.G. acknowledges support by the German Science Foundation (DFG) through the SPP 1191 "Ionic Liquids". A.B. would like to thank Fonds der Chemischen Industrie (FCI) for a graduate fellowship.

■ ABBREVIATIONS

AMP, antimicrobial peptide; CF, 5,6-carboxyfluorescein; [C_nC_{1im}], *n*-alkyl-3-methylimidazolium cation; DIC, *N*,*N*′-diisopropylcarbodiimide; DIPEA, *N*,*N*-diisopropylethylamine; DOPC, 1,2,-dioleoyl-*sn*-glycero-3-phosphocholine; DOPE, 1,2-dioleoyl-*sn*-glycero-3-phosphoethanolamine; Fmoc, fluorenylmethoxycarbonyl; GUV, giant unilamellar vesicle; HATU, 1-[bis(dimethylamino)methylene]-1*H*-1,2,3-triazolo[4,5-*b*]-pyridinium 3-oxid hexafluorophosphate; IL, ionic liquid; MIC, minimal inhibitory concentration; MRSA, methicillin-resistant *Staphylococcus aureus*; SI, selectivity index; SPPS, solid phase peptide synthesis; *t*Bu, *tert*-butyl; VRE, vancomycin-resistant enterococci.

■ REFERENCES

(1) Splith, K., and Neundorf, I. (2011) Antimicrobial peptides with cell-penetrating peptide properties and vice versa. *Eur. Biophys. J. Biophys. Lett. 40*, 387−397.

(2) Brogden, K. A. (2005) Antimicrobial peptides: pore formers or metabolic inhibitors in bacteria? *Nat. Rev. Microbiol 3*, 238−50.

(3) Koczulla, A. R., and Bals, R. (2003) Antimicrobial peptides - Current status and therapeutic potential. *Drugs 63*, 389−406.

(4) Boman, H. G. (2000) Innate immunity and the normal microflora. *Immunol. Rev. 173*, 5−16.

(5) Lai, Y. P., and Gallo, R. L. (2009) AMPed up immunity: how antimicrobial peptides have multiple roles in immune defense. *Trends Immunol. 30*, 131−141.

(6) Powers, J. P. S., and Hancock, R. E. W. (2003) The relationship between peptide structure and antibacterial activity. *Peptides 24*, 1681−1691.

(7) Melo, M. N., Ferre, R., and Castanho, M. A. R. B. (2009) OPINION Antimicrobial peptides: linking partition, activity and high membrane-bound concentrations. *Nat. Rev. Microbiol. 7*, 245−250.

(8) Sang, Y. M., Ross, C. R., Rowland, R. R. R., and Blecha, F. (2008) Toll-like receptor 3 activation decreases porcine arterivirus infection. *Viral Immunol. 21*, 303−313.
(9) Wimley, W. C., and Hristova, K. (2011) Antimicrobial peptides: successes, challenges and unanswered questions. *J. Membr. Biol. 239*, 27−34.
(10) Beckloff, N., Laube, D., Castro, T., Furgang, D., Park, S., Perlin, D., Clements, D., Tang, H., Scott, R. W., Tew, G. N., and Diamond, G. (2007) Activity of an antimicrobial peptide mimetic against planktonic and biofilm cultures of oral pathogens. *Antimicrob. Agents Chemother. 51*, 4125−4132.
(11) Huang, H. W. (2000) Action of antimicrobial peptides: two-state model. *Biochemistry 39*, 8347−52.
(12) Song, Y. M., Park, Y., Lim, S. S., Yang, S. T., Woo, E. R., Park, I. S., Lee, J. S., Kim, J. I., Hahm, K. S., Kim, Y., and Shin, S. Y. (2005) Cell selectivity and mechanism of action of antimicrobial model peptides containing peptoid residues. *Biochemistry 44*, 12094−12106.
(13) Rapaport, D., and Shai, Y. (1991) Interaction of fluorescently labeled pardaxin and its analogs with lipid bilayers. *J. Biol. Chem. 266*, 23769−23775.
(14) Ludtke, S. J., He, K., Heller, W. T., Harroun, T. A., Yang, L., and Huang, H. W. (1996) Membrane pores induced by magainin. *Biochemistry 35*, 13723−13728.
(15) Gazit, E., Miller, I. R., Biggin, P. C., Sansom, M. S. P., and Shai, Y. (1996) Structure and orientation of the mammalian antibacterial peptide cecropin P1 within phospholipid membranes. *J. Mol. Biol. 258*, 860−870.
(16) Ostolaza, H., Bartolome, B., Dezarate, I. O., Delacruz, F., and Goni, F. M. (1993) Release of lipid vesicle contents by the bacterial protein toxin alpha-hemolysin. *Biochim. Biophys. Acta 1147*, 81−88.
(17) Zasloff, M. (2002) Innate immunity, antimicrobial peptides, and protection of the oral cavity. *Lancet 360*, 1116−1117.
(18) Postleb, F., Stefanik, D., Seifert, H., and Giernoth, R. (2013) Bionic liquids: imidazolium-based ionic liquids with antimicrobial activity. *Z. Naturforsch., B 68*, 1123−1128.
(19) Larrick, J. W., Morgan, J. G., Palings, I., Hirata, M., and Yen, M. H. (1991) Complementary-DNA sequence of rabbit cap18 - a unique lipopolysaccharide binding-protein. *Biochem. Biophys. Res. Commun. 179*, 170−175.
(20) Neundorf, I., Rennert, R., Hoyer, J., Schramm, F., Löbner, K., Kitanovic, I., and Wölfl, S. (2009) Fusion of a short HA2-derived peptide sequence to cell-penetrating peptides improves cytosolic uptake, but enhances cytotoxic activity. *Pharmaceuticals 2*, 49−65.
(21) Hu, W., Splith, K., Neundorf, I., Merz, K., and Schatzschneider, U. (2012) Influence of the metal center and linker on the intracellular distribution and biological activity of organometal-peptide conjugates. *J. Biol. Inorg. Chem. 17*, 175−85.
(22) Splith, K., Hu, W., Schatzschneider, U., Gust, R., Ott, I., Onambele, L. A., Prokop, A., and Neundorf, I. (2010) Protease-activatable organometal-Peptide bioconjugates with enhanced cytotoxicity on cancer cells. *Bioconjugate Chem. 21*, 1288−96.
(23) Splith, K., Bergmann, R., Pietzsch, J., and Neundorf, I. (2012) Specific targeting of hypoxic tumor tissue with nitroimidazole-peptide conjugates. *ChemMedChem 7*, 57−61.
(24) Richter, S., Bouvet, V., Wuest, M., Bergmann, R., Steinbach, J., Pietzsch, J., Neundorf, I., and Wuest, F. (2012) ^{18}F-Labeled phosphopeptide-cell-penetrating peptide dimers with enhanced cell uptake properties in human cancer cells. *Nucl. Med. Biol. 39*, 1202−12.
(25) Agerberth, B., Gunne, H., Odeberg, J., Kogner, P., Boman, H. G., and Gudmundsson, G. H. (1995) Fall-39, a putative human peptide antibiotic, is cysteine-free and expressed in bone-marrow and testis. *Proc. Natl. Acad. Sci. U.S.A. 92*, 195−199.
(26) Oren, Z., Lerman, J. C., Gudmundsson, G. H., Agerberth, B., and Shai, Y. (1999) Structure and organization of the human antimicrobial peptide LL-37 in phospholipid membranes: relevance to the molecular basis for its non-cell-selective activity. *Biochem. J. 341*, 501−513.
(27) Colonna, M., Berti, C., Binassi, E., Fiorini, M., Sullalti, S., Acquasanta, F., Vannini, M., Di Gioia, D., Aloisio, I., Karanam, S., and Brunelle, D. J. (2012) Synthesis and characterization of imidazolium telechelic poly(butylene terephthalate) for antimicrobial applications. *React. Funct. Polym. 72*, 133−141.
(28) Xiao, L., Lv, D., and Wu, W. (2011) Brønsted acidic ionic liquids mediated metallic salts catalytic system for the chemical fixation of carbon dioxide to form cyclic carbonates. *Catal. Lett. 141*, 1838−1844.
(29) Spengler, J., Jimenez, J. C., Burger, K., Giralt, E., and Albericio, F. (2005) Abbreviated nomenclature for cyclic and branched homo- and hetero-detic peptides. *J. Pept. Res. 65*, 550−5.
(30) Manning, M. C., and Woody, R. W. (1991) Theoretical Cd studies of polypeptide helices - examination of important electronic and geometric factors. *Biopolymers 31*, 569−586.
(31) Andrews, J. M. (2001) Determination of minimum inhibitory concentrations. *J. Antimicrob. Chemother. 48* (Suppl1), 5−16.
(32) Lin, J., Wolff, T., Erickson, A., and Francis, D. (2009) Effect of bacitracin on tetracycline resistance in Escherichia coli and Salmonella. *Veterinary Microbiology 138*, 353−60.
(33) Rosato, A., Piarulli, M., Corbo, F., Muraglia, M., Carone, A., Vitali, M. E., and Vitali, C. (2010) In vitro synergistic antibacterial action of certain combinations of gentamicin and essential oils. *Curr. Med. Chem. 17*, 3289−95.
(34) Camacho-Corona Mdel, R., Ramirez-Cabrera, M. A., Santiago, O. G., Garza-Gonzalez, E., Palacios Ide, P., and Luna-Herrera, J. (2008) Activity against drug resistant-tuberculosis strains of plants used in Mexican traditional medicine to treat tuberculosis and other respiratory diseases. *Phytotherapy Research 22*, 82−5.
(35) Pernak, J., Sobaszkiewicz, K., and Mirska, I. (2003) Anti-microbial activities of ionic liquids. *Green Chem. 5*, 52−56.
(36) Ryan, K. J., Ray, C. G., and Sherris, J. C. (2004) *Sherris medical microbiology: an introduction to infectious diseases*, 4th ed., McGraw-Hill, New York.
(37) Chen, Y., Guarnieri, M. T., Vasil, A. I., Vasil, M. L., Mant, C. T., and Hodges, R. S. (2007) Role of peptide hydrophobicity in the mechanism of action of alpha-helical antimicrobial peptides. *Antimicrob. Agents Chemother. 51*, 1398−406.
(38) Brender, J. R., McHenry, A. J., and Ramamoorthy, A. (2012) Does cholesterol play a role in the bacterial selectivity of antimicrobial peptides? *Front. Immunol. 3*, 195.
(39) van Zwieten, R., Bochem, A. E., Hilarius, P. M., van Bruggen, R., Bergkamp, F., Hovingh, G. K., and Verhoeven, A. J. (2012) The cholesterol content of the erythrocyte membrane is an important determinant of phosphatidylserine exposure. *Biochim. Biophys. Acta 1821*, 1493−500.
(40) McHenry, A. J., Sciacca, M. F., Brender, J. R., and Ramamoorthy, A. (2012) Does cholesterol suppress the antimicrobial peptide induced disruption of lipid raft containing membranes? *Biochim. Biophys. Acta 1818*, 3019−24.
(41) Eloff, J. N. (1998) A sensitive and quick microplate method to determine the minimal inhibitory concentration of plant extracts for bacteria. *Planta Med. 64*, 711−713.
(42) Horger, K. S., Estes, D. J., Capone, R., and Mayer, M. (2009) Films of agarose enable rapid formation of giant liposomes in solutions of physiologic ionic strength. *J. Am. Chem. Soc. 131*, 1810−9.
(43) Katayama, S., Nakase, I., Yano, Y., Murayama, T., Nakata, Y., Matsuzaki, K., and Futaki, S. (2013) Effects of pyrenebutyrate on the translocation of arginine-rich cell-penetrating peptides through artificial membranes: recruiting peptides to the membranes, dissipating liquid-ordered phases, and inducing curvature. *Biochim. Biophys. Acta 1828*, 2134−42.